ELSEVIER

Physics of the Earth and Planetary Interiors 119 (2000) 75–97

PHYSICS OF THE EARTH AND PLANETARY INTERIORS

www.elsevier.com/locate/pepi

Comparison of Accuracy and Efficiency of Time-domain Schemes for Calculating Synthetic Seismograms

Hiromitsu Mizutani *, Robert J. Geller, Nozomu Takeuchi [1]

Department of Earth and Planetary Physics, Faculty of Science, Tokyo University, Hongo 7-3-1, Bunkyo-ku, Tokyo 113-0033, Japan

Abstract

We conduct numerical experiments for several simple models to illustrate the advantages and disadvantages of various schemes for computing synthetic seismograms in the time domain. We consider both schemes that use the pseudo-spectral method (PSM) to compute spatial derivatives and schemes that use the finite difference method (FDM) to compute spatial derivatives. We show that schemes satisfying the criterion for optimal accuracy of Geller and Takeuchi (1995) are significantly more cost-effective than non-optimally accurate schemes of the same type. We then compare optimally accurate PSM schemes to optimally accurate FDM schemes. For homogeneous or smoothly varying heterogeneous media, PSM schemes require significantly fewer grid points per wavelength than FDM schemes, and are thus more cost-effective. In contrast, we show that FDM schemes are more cost-effective for media with sharp boundaries or steep velocity gradients. Thus FDM schemes appear preferable to PSM schemes for practical seismological applications. We analyze the solution error of various schemes and show that widely cited Lax-Wendroff PSM or FDM schemes that are frequently referred to as higher order schemes are in fact equivalent to second-order optimally accurate PSM or FDM schemes implemented as two-step (predictor-corrector) schemes. The error of solutions obtained using such schemes is thus second-order, rather than fourth-order.

Keywords: Time-domain scheme; Synthetic seismograms; Pseudospectral method; Finite difference method

1. Introduction

Analyses of seismic data to determine earth structure and seismic source parameters require accurate and efficient methods for computing synthetic seismograms. Many methods are available for computing synthetics, and users would like to know which method is ''best.'' However, this question does not have a single simple answer, because the accuracy and efficiency of these methods depend both on the nature of the problem and the computational equipment being used. Nevertheless, the simple numerical examples presented in this paper provide insights into the comparative advantages and disadvantages of various methods.

Only time-domain schemes are considered in this paper. Generally speaking, time-domain methods are preferable for problems requiring broad-band syn-

* Corresponding author. Fax: +81-3-5841-8791.
E-mail address: miju@solid.eps.s.u-tokyo.ac.jp (H. Mizutani).
[1] Present address: Earthquake Research Institute, Tokyo University, Yayoi 1-1-1, Bunkyo-ku, Tokyo 113-0032, Japan.

0031-9201/00/$ - see front matter
PII: S0165-1765(99)00237-2

thetics for a short time duration, whereas frequency-domain methods are preferable for long time durations and relatively narrow bandwidths. However a detailed comparison of time-domain and frequency-domain methods is outside the scope of this paper.

Time domain schemes for computation of synthetic seismograms discretize the spatial and temporal derivatives in the elastic equation of motion. Several widely used schemes are based on the finite difference method (FDM). Other schemes use the pseudospectral method (PSM) to compute spatial derivatives (e.g. Kosloff and Baysal, 1982).

In most previous studies, the accuracy of numerical schemes has been quantified by the phase velocity (or the group velocity) error, which can be derived only for a monochromatic plane wave propagating in a homogeneous structure (e.g. Fornberg, 1987; Daudt et al., 1989). On the basis of such studies, PSM schemes have been concluded to be superior to FDM schemes. However, by using the error of the numerical solution rather than the phase velocity error as the criterion for the accuracy of numerical schemes, we can evaluate their relative performance for general heterogeneous media, rather than just for the homogeneous case.

Geller and Takeuchi (1995), hereafter referred to as GT95, derived a general theory for evaluating the solution error of synthetic seismograms by using a normal mode expansion, and used this result to derive a general criterion for optimally accurate[2] numerical operators. This criterion has been used to derive optimally accurate operators in the frequency domain for laterally homogeneous (Cummins et al., 1994; Takeuchi et al., 1996) and laterally heterogeneous (Cummins et al., 1997) media in spherical coordinates. Geller and Takeuchi (1998), hereafter referred to as GT98, used the above general criterion to derive optimally accurate operators for a second-order time-domain FDM scheme for 1-D problems. Takeuchi and Geller (2000), hereafter referred to as TG00, extended these results to derive optimally accurate second-order time-domain FDM operators for 2-D and 3-D problems.

[2] ‘‘Optimally accurate’’ denotes a scheme that achieves the best possible performance for a given spatial and temporal gridding and for a given type of scheme (e.g. 2nd order FDM).

2. Theoretical Background

2.1. Criteria for optimally accurate operators

We briefly review and summarize key results of GT95. They used a normal mode expansion to derive a general result (their eq. 2.20) for estimating the relative error of synthetic seismograms in the frequency domain:

$$\text{Relative error} = \left|\frac{\text{error}}{\text{synthetic}}\right| \approx \left|\frac{\omega^2\delta T_{mm} - \delta H_{mm}}{\omega^2 - \omega_m^2}\right| = |\delta T_{mm}|\left|\frac{\omega^2 - \delta H_{mm}/\delta T_{mm}}{\omega^2 - \omega_m^2}\right|, \quad (1)$$

where ω_m is the eigenfrequency of the mode closest to the frequency ω, δT_{mm} and δH_{mm} are the matrix elements (in the normal mode basis) for the error of the numerical operators for the mass and stiffness matrices respectively, and the modes are normalized so that

$$\mathbf{u}_m^* \mathbf{H}^{\text{exact}} \mathbf{u}_n = \omega_m^2 \mathbf{u}_m^* \mathbf{T}^{\text{exact}} \mathbf{u}_n = \omega_m^2 \delta_{mn}. \quad (2)$$

As ω approaches ω_m (ω will never be equal to ω_m if ω is real and ω_m includes an imaginary part due to anelastic attenuation.), the quotient in eq. (1) will greatly increase (i.e. the relative error of the synthetic seismograms will greatly worsen), unless the following condition is approximately satisfied:

‘‘Generalized phase velocity error’’

$$= 2\,\omega_m\,\delta\omega_m = \omega_m^2\,\delta T_{mm} - \delta H_{mm} \approx 0, \quad (3)$$

where $\delta\omega_m$ is the error in the eigenfrequencies that would be obtained using the numerical operators. Note that throughout this paper the equal sign implies equality to the lowest relevant order, rather than exact equality.

Eq. (3) is the general criterion of GT95 for optimally accurate operators. If eq. (3) is satisfied, then, from eq. (1), the relative error of the synthetics is given by

$$\text{Relative error} \approx |\delta T_{mm}|. \quad (4)$$

Although the above results are all given in the frequency domain, they can readily be used to derive optimally accurate operators in the time domain (GT98, TG00). Note that it is not necessary to know the actual numerical values of the eigensolutions in order to use eq. (1) to derive optimally accurate FDM operators for heterogeneous media (see GT95, GT98 and TG00 for details). On the other hand, it is necessary to know the eigensolutions to rigorously evaluate eq. (4) for a heterogeneous medium. However, experience suggest that reasonable error estimates for second order schemes can be obtained by evaluating eq. (4) for a homogeneous medium whose properties are the effective average of those of the heterogeneous medium.

2.2. Characterizing the accuracy of numerical schemes

The following two important implications of the above results are discussed in detail by GT95. (1) It is not the error of the respective numerical operators that controls the error of the numerical solutions, but rather only that component of the error that projects onto the normal mode(s) near the frequency of interest. This means that a large ‘‘point-source’’ error at an internal or external boundary will not be a serious problem, as it will contribute only marginally to any one mode. (2) The important quantity governing whether or not a given numerical scheme is optimally accurate is not the errors of the mass and stiffness matrices individually, but rather the difference of these quantities as given in eq. (3). If the generalized phase velocity error, $\omega_m \delta\omega_m$ is zero (to lowest order) for all modes, then the numerical scheme under consideration is optimally accurate.

Much confusion exists regarding the order of accuracy of various numerical schemes. The quantity defined in eq. (3), $\omega_m \delta\omega_m$, is essentially a generalization of the error of the phase velocity to the case of an arbitrarily heterogeneous medium. Suppose $\omega_m^2 \delta T_{mm}$ and δH_{mm} each contain terms proportional to Δt^2 and Δx^2, where Δt and Δx are respectively the temporal and spatial grid spacing. Optimal accuracy will be achieved when these terms are equal to both $O(\Delta t^2)$ and $O(\Delta x^2)$, so that the generalized phase velocity error, $\omega_m \delta\omega_m$, as given by eq. (3) will be fourth-order, i.e. $O(\Delta t^4)$, $O(\Delta x^4)$, and $O(\Delta x^2 \Delta t^2)$. However, even though the generalized phase velocity error of the optimally accurate scheme is fourth-order, the error of the numerical solutions for the optimally accurate scheme, as given by eq. (4), will still be $O(\Delta t^2)$ and $O(\Delta x^2)$, i.e., second-order, not fourth-order. For non-optimally accurate schemes eq. (1) shows that the error of the numerical solutions will also be $O(\Delta t^2)$ and $O(\Delta x^2)$, but will be multiplied by a dimensionless amplification factor on the order of

$$\left| \frac{\omega^2 - \delta H_{mm} / \delta T_{mm}}{\omega^2 - \omega_m^2} \right|. \tag{5}$$

3. PSM-FDM operators for 1-D case

In this paper, for simplicity, we consider only the 1-D case but the general approach followed here can also be applied to the 2-D and 3-D cases (see Appendix). The strong form of the elastic equation of motion (See Geller and Ohminato, 1994, for a definitions of the strong and weak forms of the elastic equation of motion.) for the 1-D case in the time domain is as follows:

$$\rho(x) \frac{\partial^2 u(x,t)}{\partial t^2} - \frac{\partial}{\partial x}\left(\mu(x) \frac{\partial u(x,t)}{\partial x} \right) = f(x,t), \tag{6}$$

where ρ is the density, μ is the rigidity, u is the displacement, and f is the external body force. Throughout this paper the elastic moduli are purely real.

The following well known scheme (e.g. Kosloff and Baysal, 1982) uses a second order FDM operator for temporal differentiation, and a Fourier difference (pseudo-spectral) operator for spatial differentiation. (We refer to this as the conventional PSM-FDM scheme.)

$$\begin{aligned} \rho_j \frac{u_j^{n+1} - 2u_j^n + u_j^{n-1}}{\Delta t^2} &= (\mathcal{F}^{-1} ik\mathcal{F})\mu_j (\mathcal{F}^{-1} ik\mathcal{F}) u_j^n + f_j^n \\ &= [\mathcal{D} u_j \mathcal{D}] u_j^n + f_j^n, \end{aligned} \tag{7}$$

where Δt is the temporal grid interval, and Δx is the spatial grid interval. u_j^n is the displacement at time $t = n\Delta t$ and at spatial coordinate $x = j\Delta x$, ρ_j

is the density at $x = j\Delta x$, μ_j is the rigidity at $x = j\Delta x$, and $\mathcal{D}$ is the Fourier difference operator:

$$\mathcal{D} = \mathcal{F}^{-1} ik \mathcal{F}, \tag{8}$$

where $\mathcal{F}$ represents a discrete Fourier transform operator for spatial differentiation, $\mathcal{F}^{-1}$represents an inverse discrete Fourier transform operator, and k is the wavenumber. The Fourier and inverse Fourier transform operators used in this paper are normalized so that

$$\mathcal{F}^{-1}\mathcal{F}u_j^n = \mathcal{F}\mathcal{F}^{-1}u_j^n = u_j^n. \tag{9}$$

3.1. Computation of derivatives

It is well known (e.g., Witte and Richards, 1990, Fornberg, 1990, Özdenvar and McMechan, 1996) that Fourier derivative operators achieve greater accuracy by computing the spatial derivatives at $x = (n+1/2)\Delta x$ rather than at $x = n\Delta x$. This is accomplished by using the discrete equivalent of the shift theorem, i.e. multiplying in the wavenumber domain by $\exp(ik\Delta x/2)$, where k is the discrete wavenumber and $i = \sqrt{-1}$, for the first spatial differentiation, and shifting back by multiplying by $\exp(-ik\Delta x/2)$ in the wavenumber domain for the second spatial differentiation. In other words, eq. (8) is replaced by

$$\mathcal{D} = \mathcal{F}^{-1} ik \exp(ik\Delta x/2)\mathcal{F} \tag{10}$$

for the first of the differentiations in eq. (2) and by

$$\mathcal{D} = \mathcal{F}^{-1} ik \exp(-ik\Delta x/2)\mathcal{F} \tag{11}$$

for the second differentiation.

Our derivation of optimally accurate PSM-FDM operators (below) is applicable to either of the above definitions (eq. 3 or eqs. 5 and 6) of the derivative operators. We use the staggered derivatives in the numerical examples.

3.2. Conventional and optimally accurate PSM-FDM operators

We write the conventional PSM-FDM elastic equation of motion in matrix form as follows:

$$(\mathbf{A}^0 - \mathbf{K}^0)\mathbf{u}^0 = \mathbf{f}. \tag{12}$$

In this paper $\mathbf{A}^0$ and $\mathbf{K}^0$ respectively denote the conventional temporal and spatial derivative operators rather than the exact operators, and $\mathbf{u}^0$ denotes the solution computed using the conventional operators rather than the exact solution. The conventional operators are written as difference stencils as follows:

$$\mathbf{A}^0 = \left(\frac{\rho_j}{\Delta t^2}\right) \times \begin{array}{|c|c|} \hline & x \\ \hline t+\Delta t & 1 \\ t & -2 \\ t-\Delta t & 1 \\ \hline \end{array} \tag{13}$$

$$\mathbf{K}^0 = \begin{array}{|c|c|} \hline & x \\ \hline t+\Delta t & \\ t & \mathcal{D}\mu_j\mathcal{D} \\ t-\Delta t & \\ \hline \end{array}\ , \tag{14}$$

with the blank spaces in the stencil for $\mathbf{K}^0$ (eq. 9) denoting zeros. This convention is followed throughout this paper. Eq. (7), the conventional PSM-FDM scheme, is a system of simultaneous linear equations in which the unknowns are the displacements at the next time step. As each equation contains only a single unknown, it is easy to solve explicitly for the displacements at time $t + \Delta t$.

The error of the conventional operators is computed by a Taylor series expansion. Omitting details, we obtain the following results:

$$\delta\mathbf{A}^0\ \mathbf{u}^0 = (\mathbf{A}^0 - \mathbf{A}^{\text{exact}})\mathbf{u}^0 = \rho\frac{\Delta t^2}{12}\frac{\partial^4 u}{\partial t^4} \tag{15}$$

$$\delta\mathbf{K}^0\ \mathbf{u}^0 = (\mathbf{K}^0 - \mathbf{K}^{\text{exact}})\mathbf{u}^0 = 0, \tag{16}$$

where $\mathbf{A}^{\text{exact}}$ and $\mathbf{K}^{\text{exact}}$ are the exact temporal and spatial operators. Eq. (15) gives the error due to the FDM time differentiation, while eq. (16) shows that the PSM spatial differentiation is essentially exact (neglecting the possibility of errors due to aliasing). Combining these two results, we obtain the time-domain error of the conventional PSM-FDM operators:

$$(\delta\mathbf{A}^0 - \delta\mathbf{K}^0)\mathbf{u} = \rho\frac{\Delta t^2}{12}\frac{\partial^4 u}{\partial t^4}. \tag{17}$$

To satisfy the criterion for optimally accurate operators (see GT95 and GT98 for definitions and derivations), we must derive operators $\mathbf{A}'$ and $\mathbf{K}'$ which, rather than eq. (17), instead have the following errors:

$$\boldsymbol{\delta}\mathbf{A}'\mathbf{u}^0 = (\mathbf{A}' - \mathbf{A}^{\text{exact}})\mathbf{u}^0 = \rho\frac{\Delta t^2}{12}\frac{\partial^4 u}{\partial t^4}$$
$$\boldsymbol{\delta}\mathbf{K}'\mathbf{u}^0 = (\mathbf{K}' - \mathbf{K}^{\text{exact}})\mathbf{u}^0 = \frac{\Delta t^2}{12}\frac{\partial^2}{\partial t^2}\left(\frac{\partial}{\partial x}\mu\frac{\partial u}{\partial x}\right). \tag{18}$$

Combining the above results, the time-domain error of the optimally accurate scheme is

Time-domain error =

$$(\boldsymbol{\delta}\mathbf{A}' - \boldsymbol{\delta}\mathbf{K}')\mathbf{u} = \frac{\Delta t^2}{12}\frac{\partial^2}{\partial t^2}\left[\rho\frac{\partial^2 u}{\partial t^2} - \frac{\partial}{\partial x}\left(\mu\frac{\partial u}{\partial x}\right)\right]$$
$$= \frac{\Delta t^2}{12}\rho\frac{\partial^4 u}{\partial t^4} - \frac{\Delta t^2}{12}\frac{\partial^2}{\partial t^2}\frac{\partial}{\partial x} \times\left(\mu\frac{\partial u}{\partial x}\right). \tag{19}$$

The first line of eq. (19) shows that the desired time domain error of the optimally accurate schemes is given by derivatives of the left-hand side (l.h.s.) of the equation of motion (eq. 6). The bracketed term in the first line of eq. (19) will thus be zero when $u(x,t)$ is a normal mode, since normal modes are solutions of the homogeneous equation of motion. We construct numerical operators that have the desired time-domain error using the second line of eq. (19). Omitting the details of the derivation, the optimally accurate operators that yield errors of the form of eq. (19) are as follows:

$$\mathbf{A}' = \mathbf{A}^0 \tag{20}$$

$$\mathbf{K}' = \begin{array}{c|c|} & x \\ \hline t+\Delta t & \frac{1}{12}\mathcal{D}\mu_j\mathcal{D} \\ t & \frac{10}{12}\mathcal{D}\mu_j\mathcal{D} \\ t-\Delta t & \frac{1}{12}\mathcal{D}\mu_j\mathcal{D} \\ \hline \end{array}\ . \tag{21}$$

Eq. (20) shows that the temporal derivative operator is unchanged, while eq. (21) shows that the spatial derivative operator is ''blurred'' into the temporal domain. The extension of this result to the 2-D and 3-D case is straightforward (see Appendix).

3.3. Predictor-Corrector scheme

The optimally accurate operators given in eqs. (20) and (21) yield the following implicit scheme:

$$(\mathbf{A}' - \mathbf{K}')\mathbf{u} = \mathbf{f}. \tag{22}$$

To avoid the need to solve a system of linear equations at each time step, we use the same type of predictor-corrector scheme as GT98. We rewrite eq. (22) as follows:

$$\left[(\mathbf{A}^0 + \boldsymbol{\delta}\mathbf{A}) - (\mathbf{K}^0 + \boldsymbol{\delta}\mathbf{K})\right](\mathbf{u}^0 + \boldsymbol{\delta}\mathbf{u}) = \mathbf{f}, \tag{23}$$

where we represent the optimally accurate operators $\mathbf{A}'$ and $\mathbf{K}'$ as the sum of the conventional operator and a correction term:

$$\mathbf{A}' = \mathbf{A}^0 + \boldsymbol{\delta}\mathbf{A}$$
$$\mathbf{K}' = \mathbf{K}^0 + \boldsymbol{\delta}\mathbf{K}, \tag{24}$$

where

$$\boldsymbol{\delta}\mathbf{K} = \begin{array}{c|c|} & x \\ \hline t+\Delta t & \frac{1}{12}\mathcal{D}\mu_j\mathcal{D} \\ t & -\frac{2}{12}\mathcal{D}\mu_j\mathcal{D} \\ t-\Delta t & \frac{1}{12}\mathcal{D}\mu_j\mathcal{D} \\ \hline \end{array} \tag{25}$$

and

$$\boldsymbol{\delta}\mathbf{A} = 0. \tag{26}$$

Note that the corrector operators $\boldsymbol{\delta}\mathbf{A}$ and $\boldsymbol{\delta}\mathbf{K}$ are distinct from the operator errors $\boldsymbol{\delta}\mathbf{A}'$ and $\boldsymbol{\delta}\mathbf{K}'$ that are defined in eq. (18).

The predictor-corrector scheme is implemented as follows. First, the predictor term is computed using the conventional operators by solving eq. (12). The corrector term is then computed using the first order Born approximation:

$$(\mathbf{A}^0 - \mathbf{K}^0)\boldsymbol{\delta}\mathbf{u} = -(\boldsymbol{\delta}\mathbf{A} - \boldsymbol{\delta}\mathbf{K})\mathbf{u}^0. \tag{27}$$

The solution of eq. (22) at time $t+\Delta t$ is the sum of the predictor term and the corrector term:

$$\mathbf{u} = \mathbf{u}^0 + \boldsymbol{\delta}\mathbf{u}. \tag{28}$$

Note that $\boldsymbol{\delta}\mathbf{u}(t) = \boldsymbol{\delta}\mathbf{u}(t-\Delta t) = 0$, as $\mathbf{u}(t)$ and $\mathbf{u}(t-\Delta t)$ will already have been corrected by applications of eq. (28) at previous time steps. The computation specified in eq. (27) can therefore be simplified to

$$\mathbf{A}^0 \ \boldsymbol{\delta}\mathbf{u} = \boldsymbol{\delta}\mathbf{K} \ \mathbf{u}^0, \tag{29}$$

where the difference stencil for eq. (29) is

$$\frac{\rho_j}{\Delta t^2} \begin{array}{|c|c|} \hline & x \\ \hline t+\Delta t & 1 \\ t & -2 \\ t-\Delta t & 1 \\ \hline \end{array} \ \boldsymbol{\delta}\mathbf{u} = \begin{array}{|c|c|} \hline & x \\ \hline t+\Delta t & \frac{1}{12}\mathcal{D}\mu_j\mathcal{D} \\ t & -\frac{2}{12}\mathcal{D}\mu_j\mathcal{D} \\ t-\Delta t & \frac{1}{12}\mathcal{D}\mu_j\mathcal{D} \\ \hline \end{array} \ \mathbf{u}^0 \, . \tag{30}$$

As noted above, $\boldsymbol{\delta}\mathbf{u}(t) = \boldsymbol{\delta}\mathbf{u}(t - \Delta t) = 0$. The l.h.s. of eq. (30) therefore becomes

$$\frac{\rho_j}{\Delta t^2} \boldsymbol{\delta}\mathbf{u}(t + \Delta t). \tag{31}$$

The right-hand side (r.h.s.) of eq. (30) requires Fourier (FFT) spatial difference operations at times $t + \Delta t$, t and $t - \Delta t$. But the last two will already have been computed at previous time steps, so if we store these results temporarily, we only have to compute the Fourier difference $(\mathcal{D}\mu_j\mathcal{D})\mathbf{u}^0$ for time $t + \Delta t$. Thus, the above optimally accurate PSM-FDM scheme requires twice as many Fourier differentiations and about three times as many additions as the conventional PSM-FDM scheme. We show below that the gain in accuracy makes these additional computations highly worthwhile.

3.4. Solution error

We derive the solution error of the conventional (eqs. 12–14) and the optimally accurate PSM-FDM scheme (eqs. 20–22) following GT98. To evaluate the solution error, we define the frequency domain operators corresponding to the conventional time-domain PSM-FDM operators (eq. 12):

$$(\mathbf{B}^0 - \mathbf{L}^0)\mathbf{u}^0 = \mathbf{f}, \tag{32}$$

where $\mathbf{B}^0$ and $\mathbf{L}^0$ are the frequency domain operators which correspond to $\mathbf{A}^0$ and $\mathbf{K}^0$ in the time domain. In this paper the Fourier transform is defined as follows:

$$\mathbf{u}(\omega) = \int_{-\infty}^{\infty} \exp(i\omega t)\mathbf{u}(t)\,dt. \tag{33}$$

Following GT95, the equation of motion in the frequency domain can be written in the following operator form:

$$(\omega^2 \mathbf{T}^0 - \mathbf{H}^0)\mathbf{u} = -\mathbf{f}, \tag{34}$$

where $\mathbf{T}^0$ and $\mathbf{H}^0$ are the mass and stiffness matrices, which are related to $\mathbf{B}^0$ and $\mathbf{L}^0$ as follows:

$$\begin{aligned} \omega^2 \mathbf{T}^0 &= -\mathbf{B}^0 \\ \mathbf{H}^0 &= -\mathbf{L}^0. \end{aligned} \tag{35}$$

We define the operator errors $\boldsymbol{\delta}\mathbf{B}^0$, $\boldsymbol{\delta}\mathbf{L}^0$, and $\boldsymbol{\delta}\mathbf{T}^0$, $\boldsymbol{\delta}\mathbf{H}^0$ as follows:

$$\begin{aligned} \boldsymbol{\delta}\mathbf{B}^0 &= \mathbf{B}^0 - \mathbf{B}^{\text{exact}} \\ \boldsymbol{\delta}\mathbf{L}^0 &= \mathbf{L}^0 - \mathbf{L}^{\text{exact}} \\ \boldsymbol{\delta}\mathbf{T}^0 &= \mathbf{T}^0 - \mathbf{T}^{\text{exact}} \\ \boldsymbol{\delta}\mathbf{H}^0 &= \mathbf{H}^0 - \mathbf{H}^{\text{exact}}. \end{aligned} \tag{36}$$

From eq. (30), the operator errors are related as follows:

$$\begin{aligned} \omega^2 \boldsymbol{\delta}\mathbf{T}^0 &= -\boldsymbol{\delta}\mathbf{B}^0 \\ \boldsymbol{\delta}\mathbf{H}^0 &= -\boldsymbol{\delta}\mathbf{L}^0. \end{aligned} \tag{37}$$

Using the above relations, the basic error of the conventional PSM-FDM operator is:

$$\begin{aligned} (\omega^2 \boldsymbol{\delta}\mathbf{T}^0 - \boldsymbol{\delta}\mathbf{H}^0)\mathbf{u} &= (-\boldsymbol{\delta}\mathbf{B}^0 + \boldsymbol{\delta}\mathbf{L}^0)\mathbf{u} \\ &= -\frac{\Delta t^2}{12}\omega^2 \rho \omega^2 \mathbf{u}. \end{aligned} \tag{38}$$

The optimally accurate PSM-FDM operators are (eqs. 20 and 21) $\mathbf{A}'$ and $\mathbf{K}'$ in the time domain, and their Fourier transforms are $\mathbf{B}'$ and $\mathbf{L}'$ respectively. To compute the relative solution error, we first define

$$\begin{aligned} \omega^2 \mathbf{T}' &= -\mathbf{B}' \\ \mathbf{H}' &= -\mathbf{L}'. \end{aligned} \tag{39}$$

The operator errors are then

$$\begin{aligned} \boldsymbol{\delta}\mathbf{B}' &= \mathbf{B}' - \mathbf{B}^{\text{exact}} \\ \boldsymbol{\delta}\mathbf{L}' &= \mathbf{L}' - \mathbf{L}^{\text{exact}} \\ \boldsymbol{\delta}\mathbf{T}' &= \mathbf{T}' - \mathbf{T}^{\text{exact}} \\ \boldsymbol{\delta}\mathbf{H}' &= \mathbf{H}' - \mathbf{H}^{\text{exact}}. \end{aligned} \tag{40}$$

When $\mathbf{u}$ is an eigenfunction and ω is the corresponding eigenfrequency, the basic error of the optimally accurate PSM-FDM scheme (eq. 22) is thus:

$$
\begin{aligned}
(\omega^2\boldsymbol{\delta}\mathbf{T}' - \boldsymbol{\delta}\mathbf{H}')\mathbf{u} = (-\boldsymbol{\delta}\mathbf{B}' + \boldsymbol{\delta}\mathbf{L}')\mathbf{u} \\
&= -\frac{\Delta t^2}{12}\omega^2\rho\omega^2 u \\
&\quad -\frac{\Delta t^2}{12}\omega^2\frac{\partial}{\partial x}\left(\mu\frac{\partial u}{\partial x}\right) \\
&= -\frac{\omega^2\Delta t^2}{12}[\mathrm{EQM}] = 0,
\end{aligned}
\tag{41}
$$

where $[\mathrm{EQM}]$ is the l.h.s. of the homogeneous equation of motion in the frequency domain:

$$
[\mathrm{EQM}] = \rho\omega^2 u + \frac{\partial}{\partial x}\left(\mu\frac{\partial u}{\partial x}\right),
\tag{42}
$$

so that $[\mathrm{EQM}] = 0$ when u is an eigenfunction and ω is the corresponding eigenfrequency. As eq. (41) shows that the above optimally accurate PSM-FDM scheme satisfies the general criterion of GT95, the relative solution error (from eq. 4) of the optimally accurate PSM-FDM scheme is

$$
|\delta T'_{mm}| = \frac{\omega_m^2\Delta t^2}{12}.
\tag{43}
$$

Thus, the relative solution error of the optimally accurate PSM-FDM scheme is still $O(\Delta t^2)$, even though the generalized phase velocity error (see eq. 3) is fourth-order. However, as we confirm by the numerical tests in section 6, the amplitude of the $O(\Delta t^2)$ error is much smaller for the optimally accurate PSM-FDM scheme than for the conventional PSM-FDM scheme.

3.5. Stability

The stability condition for the conventional 1-D PSM-FDM schemes was analyzed by Kosloff and Baysal (1982, p. 1412). We follow their approach to estimate the stability condition for the optimally accurate PSM-FDM schemes. For a homogeneous medium we substitute a harmonic solution, $u = \exp[i(kx - \omega t)]$, into the conventional operator (eq. 12) to obtain Kosloff and Baysal's stability condition for the conventional operators:

$$
\Delta t \le \frac{2}{\pi}\frac{\Delta x}{\beta} \approx 0.64\frac{\Delta x}{\beta},
\tag{44}
$$

where

$$
\beta = \sqrt{\mu/\rho}
\tag{45}
$$

is the wave velocity. The stability condition for the optimally accurate scheme (22) in a homogeneous medium is derived in the same way. Omitting details, we obtain:

$$
\Delta t \le \frac{\sqrt{6}}{\pi}\frac{\Delta x}{\beta} \approx 0.78\frac{\Delta x}{\beta}.
\tag{46}
$$

Thus the stability condition for the optimally accurate PSM-FDM schemes is slightly relaxed as compared to that for the conventional PSM-FDM schemes.

The stability condition for a heterogeneous medium cannot be determined analytically, but could be determined numerically on the basis of the maximum eigenvalue of the numerical operators. We have not made such estimates for either the conventional or optimally accurate PSM-FDM operators, but GT98 and TG00 made such estimates for conventional and optimally accurate time-domain FDM operators. On the basis of their results, we conjecture that eqs. (44) and (46) are approximately correct for a heterogeneous medium if the maximum value of β is used.

3.6. Numerical dispersion

In this section, we assume a homogeneous, isotropic medium whose exact phase velocity β is given by eq. (45). We substitute a harmonic solution

$$
u = \exp[ik(x - \beta^{\text{numerical}} t)].
\tag{47}
$$

into eqs. (12) and (22). After straightforward computation, we obtain the numerical phase velocity β_0

and β' for the conventional and optimally accurate schemes respectively:

$$\beta_0 = \frac{1}{k\Delta t}\cos^{-1}\left[1 - \frac{k^2\beta^2\Delta t^2}{2}\right] = \beta\left[1 + \frac{1}{24}(k\beta\Delta t)^2 + \frac{3}{640}(k\beta\Delta t)^4 + ...\right] \quad (48)$$

$$\beta' = \frac{1}{k\Delta t}\cos^{-1}\left[\frac{1 - \frac{5}{12}k^2\beta^2\Delta t^2}{1 + \frac{1}{12}k^2\beta^2\Delta t^2}\right] = \beta\left[1 + \frac{1}{480}(k\beta\Delta t)^4 + ...\right]. \quad (49)$$

Eqs. (48) and (49) show that the numerical dispersion for the conventional PSM-FDM scheme is $O(\Delta t^2)$, while that for the optimally accurate PSM-FDM scheme is $O(\Delta t^4)$. This is an expected result, since the operators for the optimally accurate scheme satisfy eq. (3), which is in turn equivalent to minimizing numerical dispersion to the lowest order.

4. Fourth order Runge-Kutta scheme

PSM spatial derivative operators are highly accurate (except for errors due to spatial aliasing), so higher order time integration schemes are often used to minimize the error due to temporal discretization. A fourth order Runge-Kutta (RK4) scheme (e.g., Fornberg, 1996, pp. 197–200) is one possible higher order time integration scheme that can be combined with a PSM spatial scheme. We refer to this combination as a PSM-RK4 scheme. Other higher order schemes have also been proposed (e.g., Tal-Ezer et al., 1987), but we do not consider them here.

In this section, we show that the conventional PSM-RK4 scheme is optimally accurate to $O(\Delta t^4)$. Following Fornberg (1996), we begin by rewriting the 1-D equation of motion (eq. 6) as a system of two coupled first order partial differential equations:

$$\frac{d\mathbf{v}}{dt} = \mathbf{D}\mathbf{v} + \mathbf{f}', \quad (50)$$

where $\mathbf{v}$ is the motion-stress vector:

$$\mathbf{v} = \begin{pmatrix} \dot{\mathbf{u}} \\ \boldsymbol{\sigma} \end{pmatrix}, \quad (51)$$

$\dot{\mathbf{u}}$ is the first derivative of the displacement with respect to time, $\mathbf{D}$ is the spatial derivative operator:

$$\mathbf{D} = \begin{pmatrix} 0 & \frac{1}{\rho}\frac{\partial}{\partial x} \\ \mu\frac{\partial}{\partial x} & 0 \end{pmatrix} = \begin{pmatrix} 0 & \frac{1}{\rho}\mathcal{D} \\ \mu\mathcal{D} & 0 \end{pmatrix}, \quad (52)$$

and $\mathbf{f}'$ is the body force vector:

$$\mathbf{f}' = \begin{pmatrix} \mathbf{f}(t)/\rho \\ 0 \end{pmatrix}. \quad (53)$$

The spatial derivatives on the r.h.s. of eq. (52) are computed using the PSM, and the time integration on the l.h.s. is computed using the following RK4 scheme:

$$\left.\begin{aligned} \mathbf{d}^{(1)} &= \Delta t\ \mathbf{D}\mathbf{v}^n + \Delta t\ \mathbf{f}'(t) \\ \mathbf{d}^{(2)} &= \Delta t\ \mathbf{D}\left(\mathbf{v}^n + \frac{1}{2}\mathbf{d}^{(1)}\right) + \Delta t\ \mathbf{f}'(t + \Delta t/2) \\ \mathbf{d}^{(3)} &= \Delta t\ \mathbf{D}\left(\mathbf{v}^n + \frac{1}{2}\mathbf{d}^{(2)}\right) + \Delta t\ \mathbf{f}'(t + \Delta t/2) \\ \mathbf{d}^{(4)} &= \Delta t\ \mathbf{D}(\mathbf{v}^n + \mathbf{d}^{(3)}) + \Delta t\ \mathbf{f}'(t + \Delta t) \end{aligned}\right\} \quad (54)$$

$$\mathbf{v}^{n+1} = \mathbf{v}^n + \frac{1}{6}\left[\mathbf{d}^{(1)} + 2\mathbf{d}^{(2)} + 2\mathbf{d}^{(3)} + \mathbf{d}^{(4)}\right], \quad (55)$$

where $\mathbf{v}^n = \mathbf{v}(n\Delta t)$. The various $\mathbf{d}^{(i)}$ are intermediate solutions. Substituting eqs. (54) and (55) into eq. (50), we obtain the following one-step explicit operator for the PSM-RK4 scheme:

$$\frac{\mathbf{v}^{n+1} - \mathbf{v}^n}{\Delta t} = \mathbf{D}\mathbf{v}^n + \frac{\Delta t}{2}\mathbf{D}^2\mathbf{v}^n + \frac{\Delta t^2}{6}\mathbf{D}^3\mathbf{v}^n + \frac{\Delta t^3}{24}\mathbf{D}^4\mathbf{v}^n + \mathbf{f}^{\mathrm{RK}}, \quad (56)$$

where $\mathbf{f}^{\mathrm{RK}}$ is the fourth order body force term for the RK4 scheme:

$$\mathbf{f}^{\mathrm{RK}} = \frac{\mathbf{f}' + 4\mathbf{f}'^{+} + \mathbf{f}'^{++}}{6} + \Delta t\mathbf{D}\frac{\mathbf{f}' + 2\mathbf{f}'^{+}}{6} + \frac{\Delta t^2}{12}\mathbf{D}^2(\mathbf{f}' + \mathbf{f}'^{+}) + \frac{\Delta t^3}{24}\mathbf{D}^3\mathbf{f}', \quad (57)$$

where

$$\begin{aligned} \mathbf{f}'^{+} &= \mathbf{f}'(t + \Delta t/2) \\ \mathbf{f}'^{++} &= \mathbf{f}'(t + \Delta t). \end{aligned} \quad (58)$$

Substituting eqs. (51) and (52) into eq. (56), we obtain the explicit form of eq. (56):

$$\rho\frac{\dot{\mathbf{u}}^{n+1}-\dot{\mathbf{u}}^{n}}{\Delta t}-\frac{\Delta t}{2}\mu\mathcal{D}^2\dot{\mathbf{u}}^n-\frac{\Delta t^2}{6}\frac{\mu}{\rho}\mathcal{D}^3\boldsymbol{\sigma}^n-\frac{\Delta t^3}{24}\frac{\mu^2}{\rho}\mathcal{D}^2\dot{\mathbf{u}}^n=\mathcal{D}\boldsymbol{\sigma}^n+\frac{\mathbf{f}+4\,\mathbf{f}^{+}+\mathbf{f}^{++}}{6}+\frac{\Delta t^2}{12}\mathcal{D}^2(\mathbf{f}+\mathbf{f}^{+}), \tag{59}$$

$$\frac{\boldsymbol{\sigma}^{+}-\boldsymbol{\sigma}}{\boldsymbol{\Delta}\mathbf{t}}-\frac{\Delta t}{2}\frac{\mu}{\rho}\mathcal{D}^2\boldsymbol{\sigma}^n-\frac{\Delta t^2}{6}\frac{\mu^2}{\rho}\mathcal{D}^3\dot{\mathbf{u}}^n-\frac{\Delta t^3}{24}\frac{\mu^2}{\rho^2}\mathcal{D}^4\boldsymbol{\sigma}^n=\mu\mathcal{D}\dot{\mathbf{u}}^n+\Delta\,t\mathcal{D}\frac{\mathbf{f}+2\,\mathbf{f}^{+}}{6}+\frac{\Delta t^3}{24}\mathcal{D}^3\mathbf{f}. \tag{60}$$

Transforming eqs. (59) and (60) into the frequency domain and using a Taylor expansion, we obtain the following:

$$\rho\omega^2\mathbf{u}-\frac{\Delta t^4}{120}\omega^6\rho\mathbf{u}=-\mathcal{D}\boldsymbol{\sigma}-\mathbf{f}, \tag{61}$$

$$\boldsymbol{\sigma}+\frac{\Delta t^4}{120}\omega^4\boldsymbol{\sigma}=\mu\mathcal{D}\mathbf{u}, \tag{62}$$

where we used the equation of motion (eq. 50) to eliminate lower order terms ($O(\Delta t)$, $O(\Delta t^2)$, and $O(\Delta t^3)$). Combining eqs. (61) and (62) to eliminate the stress $\boldsymbol{\sigma}$, we obtain the numerical operators for the RK4 scheme in the frequency domain:

$$(\omega^2\mathbf{T}^{\mathrm{RK}}-\mathbf{H}^{\mathrm{RK}})\mathbf{u}=-\mathbf{f} \tag{63}$$

where $\mathbf{T}^{\mathrm{RK}}$ and $\mathbf{H}^{\mathrm{RK}}$ are the mass and stiffness matrices for the PSM-RK4 scheme:

$$\omega^2\mathbf{T}^{\mathrm{RK}}\mathbf{u}=\rho\omega^2\mathbf{u}-\frac{\Delta t^4}{120}\omega^6\rho\mathbf{u},$$

and

$$\mathbf{H}^{\mathrm{RK}}\mathbf{u}=-\mu\mathcal{D}^2\mathbf{u}+\frac{\Delta t^4}{120}\omega^4\mu\mathcal{D}^2\mathbf{u}.$$

The operator errors of the PSM-RK4 scheme in the frequency domain are:

$$\begin{aligned}\boldsymbol{\delta}\mathbf{T}^{\mathrm{RK}}&=\mathbf{T}^{\mathrm{RK}}-\mathbf{T}^{\mathrm{exact}}\\ \boldsymbol{\delta}\mathbf{H}^{\mathrm{RK}}&=\mathbf{H}^{\mathrm{RK}}-\mathbf{H}^{\mathrm{exact}},\end{aligned} \tag{64}$$

where $\mathbf{T}^{\mathrm{exact}}$ and $\mathbf{H}^{\mathrm{exact}}$ are the exact mass and stiffness matrices. The basic error of the PSM-RK4 scheme for the *m*-th mode is thus

$$\begin{aligned}&[\text{Basic error for m-th mode}]\\ &=(\omega_m^2\boldsymbol{\delta}\mathbf{T}^{\mathrm{RK}}-\boldsymbol{\delta}\mathbf{H}^{\mathrm{RK}})\mathbf{u}_m\\ &=-\frac{\omega_m^4\Delta t^4}{120}[\rho\omega_m^2\mathbf{u}_m+\mu\mathcal{D}^2\mathbf{u}_m]\\ &=-\frac{\omega_m^4\Delta t^4}{120}[\mathrm{EQM}]=0.\end{aligned} \tag{65}$$

Thus the PSM-RK4 scheme satisfies GT95's criterion for optimally accurate numerical operators. The solution error in the frequency domain (as defined by eq. 4) is

$$\left|\delta T_{mm}^{\mathrm{RK}}\right|=\frac{\omega_m^4\Delta t^4}{120}. \tag{66}$$

The phase velocity for the PSM-RK4 scheme is obtained by substituting a harmonic solution into eq. (63). Omitting details, we obtain:

$$\beta^{\mathrm{RK4}}=\beta\left(1+O(\Delta t^6)\right). \tag{67}$$

The stability condition of the above PSM-RK4 scheme has been analyzed in many works (e.g., Fornberg, 1996, p. 199). Omitting details, for a homogeneous and unbounded medium, the stability condition is the same as that for optimally accurate PSM-FDM operators (eq. 46). We have confirmed this result by numerical tests.

5. Lax-Wendroff correction scheme

Lax-Wendroff (LW) correction schemes (Lax and Wendroff, 1964) for the elastic and acoustic cases have been presented by many authors (e.g. Dablain, 1986; Kneib and Kerner, 1993; Robertsson et al. 1994; Igel et al., 1995; Blanch and Robertsson, 1997). The basic concept of Lax-Wendroff correction is to use the equation of motion to replace temporal derivatives by spatial derivatives. For example, for the 1-D case, the LW correction is based on the following substitution:

$$\frac{\partial^2}{\partial t^2}\leftarrow\frac{1}{\rho}\frac{\partial}{\partial x}\mu\frac{\partial}{\partial x}. \tag{68}$$

If the operand of the operators in eq. (68) is an eigenmode of the homogeneous equation of motion, the left arrow in eq. (69) can be replaced by an equal sign, but generally the above substitution is not valid. However, we show below that the LW correction schemes, although apparently different in form, are essentially equivalent to the optimally accurate predictor-corrector schemes derived by GT98, TG00, and in this paper, and thus can be rigorously justified.

LW correction schemes are often described as a method for achieving higher order (e.g. $O(\Delta t^4)$ rather than $O(\Delta t^2)$) temporal accuracy, but we show below that this is not the case. Although LW correction schemes significantly reduce the amplitude of the error of the numerical solutions, they do not change the order of accuracy of the solutions, which is still $O(\Delta t^2)$.

5.1. Lax-Wendroff correction scheme for PSM-FDM

The LW scheme uses eq. (68) to correct the $O(\Delta t^2)$ temporal operator error of the conventional PSM-FDM scheme (see eq. 15) by spatial derivatives, using the following substitution:

$$\rho\frac{\Delta t^2}{12}\frac{\partial^4 u}{\partial t^4} \leftarrow \rho\frac{\Delta t^2}{12}\left(\frac{1}{\rho}\frac{\partial}{\partial x}\mu\frac{\partial}{\partial x}\right)\left(\frac{1}{\rho}\frac{\partial}{\partial x}\mu\frac{\partial}{\partial x}\right)u, \tag{69}$$

thereby obtaining the following spatial correction operator:

$$\boldsymbol{\delta}\mathbf{K}^{\mathrm{LW}}\mathbf{u} = \frac{\rho\Delta t^2}{12}\begin{array}{|c|c|}\hline & x \\ \hline t+\Delta t & \\ t & \left(\frac{1}{\rho}\mathcal{D}\mu\mathcal{D}\right)\left(\frac{1}{\rho}\mathcal{D}\mu\mathcal{D}\right) \\ t-\Delta t & \\ \hline\end{array}\;\mathbf{u}. \tag{70}$$

Using the above correction operator, the PSM-FDM-LW scheme is written as:

$$\begin{aligned}\mathbf{A}^0\mathbf{u} &= (\mathbf{K}^0 + \boldsymbol{\delta}\mathbf{K}^{\mathrm{LW}})\mathbf{u} + \mathbf{f}\\ &= \mathbf{K}^{\mathrm{LW}}\mathbf{u} + \mathbf{f},\end{aligned} \tag{71}$$

where

$$\mathbf{K}^{\mathrm{LW}} = \mathbf{K}^0 + \boldsymbol{\delta}\mathbf{K}^{\mathrm{LW}}. \tag{72}$$

In order to estimate the solution error of the PSM-FDM-LW scheme, we define the PSM-FDM-LW operators in the frequency domain, $\mathbf{B^0}$ and $\mathbf{L^{LW}}$. The operator errors, $\boldsymbol{\delta}\mathbf{B}^0$ and $\boldsymbol{\delta}\mathbf{L}^{\mathrm{LW}}$, are

$$\boldsymbol{\delta}\mathbf{B}^0 = \frac{\rho\omega^4\Delta t^2}{12} \tag{73}$$

$$\boldsymbol{\delta}\mathbf{L}^{\mathrm{LW}} = \frac{\rho\Delta t^2}{12}\left(\frac{1}{\rho}\frac{\partial}{\partial x}\mu\frac{\partial}{\partial x}\right)\left(\frac{1}{\rho}\frac{\partial}{\partial x}\mu\frac{\partial}{\partial x}\right)u. \tag{74}$$

When $\mathbf{u}$ is an eigenmode and the frequency ω is equal to the corresponding eigenfrequency, the basic error is as follows:

$$\begin{aligned}[\text{Basic error}] &= (\boldsymbol{\delta}\mathbf{B}^0 - \boldsymbol{\delta}\mathbf{L}^{\mathrm{LW}})\mathbf{u}\\ &= \frac{\rho\Delta t^2}{12}\left(\omega^2 - \frac{\partial}{\partial x}\mu\frac{\partial}{\partial x}\frac{1}{\rho}\right)[\mathrm{EQM}]\\ &= 0,\end{aligned} \tag{75}$$

where [EQM] is the l.h.s. of the homogeneous equation of motion in the frequency domain as given by eq. (42). Because the PSM-FDM-LW scheme is thus an optimally accurate scheme, we can evaluate the solution error based on eqs. (37) and (73):

$$\begin{aligned}&[\text{Solution error of PSM-FDM-LW scheme}]\\ &\quad = |\delta T_{mm}| = \frac{\omega_m^2\Delta t^2}{12}.\end{aligned} \tag{76}$$

Thus the solution error of the PSM-FDM-LW scheme is $O(\Delta t^2)$, rather than $O(\Delta t^4)$. Note that eq. (43), which gives the solution error for the optimally accurate PSM-FDM scheme, is equal to eq. (76). We show below that this is because the optimally accurate predictor-corrector PSM-FDM scheme is essentially equivalent to the PSM-FDM-LW scheme.

The numerical dispersion of the phase velocity for the PSM-FDM-LW scheme for homogeneous media is obtained by substituting a harmonic solution into eq. (71). Omitting details, we obtain the numerical phase velocity:

$$\beta^{\mathrm{LW}} = \beta\left[1 - \frac{1}{720}k^4(\beta\Delta t)^4\right]. \tag{77}$$

Note that the order of accuracy is the same as for the optimally accurate PSM-FDM scheme (see eq. 49), although the coefficient of the $O(\Delta t^4)$ term is different.

5.2. Equivalence of PSM-FDM-LW and optimally accurate PSM-FDM schemes

The optimally accurate PSM-FDM scheme (eq. 22) is a two-step (predictor-corrector) procedure. However these two steps can be combined, by replacing $\mathbf{u}^0(t+\Delta t)$ in the corrector step by its explicit value, from the predictor step, to obtain an explicit one-step formulation. The equation that yields the predictor term (eq. 12) may be written as follows:

$$\mathbf{u}^{n+1} - 2\mathbf{u}^n + \mathbf{u}^{n-1} = \Delta t^2 \left(\frac{1}{\rho} \mathcal{D} \mu \mathcal{D} \right) \mathbf{u}^n + \frac{\Delta t^2}{\rho} \mathbf{f}^n. \tag{78}$$

The corrector term (eq. 30) may be written as follows:

$$\begin{aligned} \delta\mathbf{K}\ \mathbf{u}^0 &= \frac{1}{12} \mathcal{D}\mu\mathcal{D}[\mathbf{u}^{n-1} - 2\mathbf{u}^n + \mathbf{u}^{n+1}] \\ &= \frac{\rho \Delta t^2}{12} \left(\frac{1}{\rho} \mathcal{D}\mu\mathcal{D} \right) \left(\frac{1}{\rho} \mathcal{D}\mu\mathcal{D} \right) \mathbf{u}^n \\ &\quad + \frac{\rho \Delta t^2}{12} \left(\frac{1}{\rho} \mathcal{D}\mu\mathcal{D} \right) \frac{\mathbf{f}^n}{\rho}, \end{aligned} \tag{79}$$

where we used eq. (78) in going from the first line of eq. (79) to the second.

The corrector term for the optimally accurate PSM-FDM scheme (eq. 79) is thus exactly equal (to the lowest order) to the LW correction term (eq. 70) if $\mathbf{f}^n = 0$, but will be slightly different due to the spatial derivative of the external body force term (the last term in eq. 79) if $\mathbf{f}^n \neq 0$. The optimally accurate PSM-FDM scheme implemented as a predictor-corrector scheme is thus equivalent to the PSM-FDM-LW scheme except for the slight error in the external body force term used by the latter. The difference of the body force term is $O(\Delta t^2)$, so it can be shown that this term does not significantly degrade the accuracy of the solution obtained eq. (71). (For a more detailed discussion of the treatment of the force term see section 5 of TG00). Note that the computational costs of both the PSM-FDM-LW scheme (eq. 71) and the predictor-corrector implementation of the optimally accurate PSM-FDM scheme (eqs. 12–28) are essentially the same, because the LW correction term (eq. 70) and the corrector step of the optimally accurate PSM-FDM scheme (eq. 30) both require two additional Fourier differentiations at each time step.

As shown by eq. (77), the error of the phase velocity is $O(\Delta t^4)$ for the homogeneous case. However, as shown by eq. (76), the relative error of the solution for the PSM-FDM-LW scheme is $O(\Delta t^2)$, and is equal to that of the optimally accurate PSM-FDM scheme given by, eq. (43). Thus both the PSM-FDM-LW scheme and the optimally accurate PSM-FDM scheme, which, as shown above, are essentially equivalent, should be classified as optimally accurate second order schemes rather than as ‘‘fourth-order’’ schemes.

5.3. Lax-Wendroff correction scheme for FDM schemes

So-called spatially fourth order and temporally second order (O(4,2)) FDM schemes are widely used (e.g. Kelly et al., 1976; Frankel and Clayton, 1986; Levander, 1988). Implementations which combine an LW correction scheme with a conventional O(4,2) FDM scheme (Dablain, 1986; Blanch and Robertsson, 1997) are hereafter referred to as FDM-LW schemes. Such schemes are often called O(4,4) schemes, meaning that fourth-order accuracy in both space and time is implied. We show in section 5.4 that the FDM-LW scheme is actually equivalent to an optimally accurate O(2,2) FDM scheme implemented as a two-step (predictor-corrector) scheme, and that the solution error of the so-called O(4,4) schemes is actually second order in both space and time. In this and the next sections, we consider only a one-dimensional homogeneous medium, but these results are applicable to general cases (see GT98 and TG00).

The conventional so-called O(4,2) scheme for a one-dimensional homogeneous medium is written in the following operator form:

$$(\mathbf{A}^0 - \mathbf{K}^F)\mathbf{u}^0 = \mathbf{f}, \tag{80}$$

where the difference stencils are $\mathbf{A}^0$ (eq. 13) and

$$\mathbf{K}^F = \begin{array}{|c|ccccc|} \hline t+\Delta t & & & & & \\ t & -1 & +16 & -30 & +16 & -1 \\ t-\Delta t & & & & & \\ \hline & x-2\Delta x & x-\Delta x & x & x+\Delta x & x+2\Delta x \\ \hline \end{array} \times \frac{\mu}{12\Delta x^2}. \tag{81}$$

The Lax-Wendroff correction scheme uses a spatial difference operator which is defined as follows:

$$\mathbf{K}^{\mathrm{LW4}} = \mathbf{K}^F + \boldsymbol{\delta}\mathbf{K}^{\mathrm{C}}, \tag{82}$$

where $\boldsymbol{\delta}\mathbf{K}^{\mathrm{C}}$ is the LW correction operator that modifies the operator error of eq. (15):

$$\rho\frac{\Delta t^2}{12}\frac{\partial^4 u}{\partial t^4} \leftarrow \frac{\Delta t^2}{12}\frac{\mu^2}{\rho}\frac{\partial^4 u}{\partial x^4}, \tag{83}$$

and

$$\boldsymbol{\delta}\mathbf{K}^{\mathrm{C}} = \begin{array}{|c|ccccc|} \hline t+\Delta t & & & & & \\ t & 1 & -4 & 6 & -4 & 1 \\ t-\Delta t & & & & & \\ \hline & x-2\Delta x & x-\Delta x & x & x+\Delta x & x+2\Delta x \\ \hline \end{array} \times \frac{\mathcal{C}^2}{12}\frac{\mu}{\Delta x^2}, \tag{84}$$

where $\mathcal{C}$ is the Courant number,

$$\mathcal{C} = \frac{\beta\Delta t}{\Delta x}. \tag{85}$$

Substituting eq. (84) into eq. (82), we obtain

$$\mathbf{K}^{\mathrm{LW4}} = \begin{array}{|c|ccccc|} \hline t+\Delta t & & & & & \\ t & -1+\mathcal{C}^2 & 16-4\mathcal{C}^2 & -30+6\mathcal{C}^2 & 16-4\mathcal{C}^2 & -1+\mathcal{C}^2 \\ t-\Delta t & & & & & \\ \hline & x-2\Delta x & x-\Delta x & x & x+\Delta x & x+2\Delta x \\ \hline \end{array} \times \frac{\mu}{12\Delta x^2}. \tag{86}$$

Using the above operators, the FDM-LW scheme can be written in operator form as follows:

$$\begin{aligned} \mathbf{A}^0\mathbf{u} &= \mathbf{K}^{\mathrm{LW4}}\mathbf{u} + \mathbf{f} \\ &= \mathbf{K}^F\mathbf{u} + \boldsymbol{\delta}\mathbf{K}^{\mathrm{C}}\mathbf{u} + \mathbf{f}. \end{aligned} \tag{87}$$

Omitting details, we compute the numerical dispersion of the phase velocity by substituting a harmonic solution into the above FDM-LW scheme:

$$\beta^{\mathrm{FDM\text{-}LW}} = \beta\left[1 - \frac{1}{720}k^4\left(4(\Delta x)^4 - 5(\Delta x)^2(\beta\Delta t)^2 + (\beta\Delta t)^4\right)\right]. \tag{88}$$

Although the above phase velocity error is fourth-order, we show below that the solution error for this scheme is (optimally accurate) second-order.

5.4. Equivalence of optimally accurate O(2,2) FDM scheme and FDM-LW scheme

GT98 derived an optimally accurate $O(2,2)$ FDM operator as a two-step (predictor-corrector) scheme. In this section, we derive the explicit (one-step) form of this scheme for a homogeneous medium, and show that it is essentially equal to the above LW scheme.

The conventional $O(2,2)$ FDM operator is written as follows:

$$(\mathbf{A}^0 - \mathbf{K}^0)\mathbf{u}^0 = \mathbf{f}, \tag{89}$$

where

$$\mathbf{K}^0 = \begin{array}{c|ccc|} t+\Delta t & & & \\ t & 1 & -2 & 1 \\ t-\Delta t & & & \\ \hline & x-\Delta x & x & x+\Delta x \end{array} \times \frac{\mu}{\Delta x^2} \tag{90}$$

and

$$\mathbf{A}^0 = \begin{array}{c|ccc|} t+\Delta t & & 1 & \\ t & & -2 & \\ t-\Delta t & & 1 & \\ \hline & x-\Delta x & x & x+\Delta x \end{array} \times \frac{\rho}{\Delta t^2}. \tag{91}$$

The optimally accurate $O(2,2)$ FDM operator derived by GT98 is as follows:

$$(\mathbf{A}' - \mathbf{K}')\mathbf{u} = \mathbf{f}, \tag{92}$$

where

$$\begin{aligned} \mathbf{A}' &= \mathbf{A}^0 + \delta\mathbf{A} \\ \mathbf{K}' &= \mathbf{K}^0 + \delta\mathbf{K} \end{aligned} \tag{93}$$

and

$$\delta\mathbf{A} = \begin{array}{c|ccc|} t+\Delta t & 1 & -2 & 1 \\ t & -2 & 4 & -2 \\ t-\Delta t & 1 & -2 & 1 \\ \hline & x-\Delta x & x & x+\Delta x \end{array} \times \frac{\rho}{12\Delta t^2} \tag{94}$$

$$\delta\mathbf{K} = \begin{array}{c|ccc|} t+\Delta t & 1 & -2 & 1 \\ t & -2 & 4 & -2 \\ t-\Delta t & 1 & -2 & 1 \\ \hline & x-\Delta x & x & x+\Delta x \end{array} \times \frac{\mu}{12\Delta x^2}. \tag{95}$$

The operator errors in the frequency domain, $\delta\mathbf{B}'$ and $\delta\mathbf{L}'$, are:

$$\delta\mathbf{B}'\ \mathbf{u} = \rho\frac{\omega^4\Delta t^2}{12}u + \rho\omega^2\frac{\Delta x^2}{12}\frac{\partial^2 u}{\partial x^2} \tag{96}$$

$$\delta\mathbf{L}'\ \mathbf{u} = \mu\omega^2\frac{\Delta t^2}{12}\frac{\partial^2 u}{\partial x^2} + \mu\frac{\Delta x^2}{12}\frac{\partial^4 u}{\partial x^4}. \tag{97}$$

When $\mathbf{u}$ is an eigenfunction and ω is the corresponding eigenfrequency, the basic error is given by

$$\begin{aligned} (\delta\mathbf{B}' - \delta\mathbf{L}')\mathbf{u} &= \frac{\Delta t^2}{12}\omega^2[\mathrm{EQM}] \\ &\quad - \frac{\Delta x^2}{12}\frac{\partial^2}{\partial x^2}[\mathrm{EQM}] \\ &= 0. \end{aligned} \tag{98}$$

By analogy to eq. (35), the matrix elements for the operator error are given by

$$\begin{aligned} \delta T'_{mm} &= -\frac{\omega_m^2\Delta t^2}{12} - \frac{k_m^2\Delta x^2}{12} \\ \delta H'_{mm} &= -\omega_m^4\frac{\Delta t^2}{12} - \frac{k_m^2\omega_m^2\Delta x^2}{12}, \end{aligned} \tag{99}$$

where for a homogeneous medium, the wavenumber of the m-th mode, k_m, is given by

$$k_m = \omega_m/\beta, \tag{100}$$

where β is given by eq. (45). From eqs. (4) and (99), the relative solution error of the above optimally accurate FDM scheme is $O(\Delta x^2, \Delta t^2)$.

GT98 implemented the above optimally accurate $O(2,2)$ scheme using a two-step predictor-corrector scheme. The explicit form of the predictor step is (see also appendix of GT98):

$$u_j^{n+1} - 2u_j^n + u_j^{n-1} = \frac{\Delta t^2}{\rho}(\mathbf{K}^0\mathbf{u})_j^n + \frac{\Delta t^2}{\rho}f_j^n. \tag{101}$$

The corrector term is obtained by solving:

$$(\mathbf{A}^0 - \mathbf{K}^0)\,\delta\mathbf{u} - (\delta\mathbf{A} - \delta\mathbf{K})\mathbf{u}^0. \tag{102}$$

We write the temporal correction term $\boldsymbol{\delta}\mathbf{A}\mathbf{u}^0$ in explicit form:

$$
\begin{aligned}
(\boldsymbol{\delta}\mathbf{A}\ \mathbf{u}^0)_j^n &= \frac{\rho}{12\,\Delta t^2}(\mathbf{u}^{n+1}-2\mathbf{u}^n+\mathbf{u}^{n-1})_{j+1} \\
&\quad - \frac{2\rho}{12\,\Delta t^2}(\mathbf{u}^{n+1}-2\mathbf{u}^n+\mathbf{u}^{n-1})_{j} \\
&\quad + \frac{\rho}{12\,\Delta t^2}(\mathbf{u}^{n+1}-2\mathbf{u}^n+\mathbf{u}^{n-1})_{j-1} \\
&= \frac{1}{12}(\mathbf{K}^0\mathbf{u}+\mathbf{f})_{j+1}^n - \frac{2}{12}(\mathbf{K}^0\mathbf{u}+\mathbf{f})_{j}^n \\
&\quad + \frac{1}{12}(\mathbf{K}^0\mathbf{u}+\mathbf{f})_{j-1}^n \\
&= \frac{1}{12}(\mathbf{K}^0\mathbf{u})_{j+1}^n - \frac{2}{12}(\mathbf{K}^0\mathbf{u})_{j}^n \\
&\quad + \frac{1}{12}(\mathbf{K}^0\mathbf{u})_{j-1}^n + \frac{1}{12}\frac{\Delta x^2}{\mu}(\mathbf{K}^0\mathbf{f})_{j}^n \\
&= (\boldsymbol{\delta}\mathbf{A}^E\mathbf{u})_j^n + \frac{\Delta x^2}{12\mu}(\mathbf{K}^0\mathbf{f})_{j}^n,
\end{aligned}
\tag{103}
$$

$\boldsymbol{\delta}\mathbf{A}^E$ is the explicit one-step form of $\boldsymbol{\delta}\mathbf{A}$:

$$
\boldsymbol{\delta}\mathbf{A}^E = \begin{array}{c|ccccc|}
\hline
t+\Delta t & & & & & \\
t & 1 & -4 & 6 & -4 & 1 \\
t-\Delta t & & & & & \\
\hline
 & x-2\Delta x & x-\Delta x & x & x+\Delta x & x+2\Delta x \\
\hline
\end{array} \times \frac{\mu}{12\Delta x^2}.
\tag{104}
$$

Omitting details, the explicit form of $\boldsymbol{\delta}\mathbf{K}\mathbf{u}^0$ is derived in the same way:

$$
(\boldsymbol{\delta}\mathbf{K}^0\ \mathbf{u}^0)_j^n = (\boldsymbol{\delta}\mathbf{K}^E\ \mathbf{u}^0)_j^n + \frac{\Delta t^2}{12\rho}(\mathbf{K}^0\mathbf{f})_j^n,
$$

where

$$
\begin{aligned}
\boldsymbol{\delta}\mathbf{K}^E &= \begin{array}{c|ccccc|}
\hline
t+\Delta t & & & & & \\
t & 1 & -4 & 6 & -4 & 1 \\
t-\Delta t & & & & & \\
\hline
 & x-2\Delta x & x-\Delta x & x & x+\Delta x & x+2\Delta x \\
\hline
\end{array} \times \frac{\mu}{12\Delta x^2} \times \frac{\mu}{\rho}\frac{\Delta t^2}{\Delta x^2} \\
&= \begin{array}{c|ccccc|}
\hline
t+\Delta t & & & & & \\
t & 1 & -4 & 6 & -4 & 1 \\
t-\Delta t & & & & & \\
\hline
 & x-2\Delta x & x-\Delta x & x & x+\Delta x & x+2\Delta x \\
\hline
\end{array} \times \frac{\mu}{12\Delta x^2}\mathcal{C}^2 .
\end{aligned}
\tag{105}
$$

Finally, the explicit one-step form of the predictor-corrector scheme is written as follows:

$$
\begin{aligned}
\mathbf{A}^0\mathbf{u} &= (\mathbf{K}^0 - \boldsymbol{\delta}\mathbf{A}^E)\mathbf{u} + \boldsymbol{\delta}\mathbf{K}^E\ \mathbf{u} + \mathbf{f}' \\
&= \mathbf{K}^F\mathbf{u} + \boldsymbol{\delta}\mathbf{K}^E\mathbf{u} + \mathbf{f}',
\end{aligned}
\tag{106}
$$

where $\mathbf{K}^F$ is the fourth order accurate spatial difference operator:

$$
\mathbf{K}^F = \mathbf{K}^0 - \boldsymbol{\delta}\mathbf{A}^E,
\tag{107}
$$

$\mathbf{K}^F$, $\mathbf{K}^0$, and $\boldsymbol{\delta}\mathbf{A}^E$ are given by eqs. (81), (90), and

(105) respectedly, and $\mathbf{f}'$ is the modified external force term:

$$\mathbf{f}' = \mathbf{f} - \frac{\Delta x^2}{12\mu}\mathbf{K}^0\mathbf{f} + \frac{\Delta t^2}{12\rho}\mathbf{K}^0\mathbf{f}. \tag{108}$$

The correction operator $\boldsymbol{\delta}\mathbf{K}^E$ in eq. (104) is equal to the LW correction term $\boldsymbol{\delta}\mathbf{K}^C$ (eq. 87). Thus eq. (106) is equal to the above so-called O(4,4) LW scheme (eq. 87), except for the slightly different external body force term in eq. (108). The slight difference of the force term is $O(\Delta x^2, \Delta t^2)$, so this correction does not degrade the order of the solution error. The relative solution error of both the FDM-LW scheme and the optimally accurate O(2,2) FDM scheme, which are basically equal, is therefore $O(\Delta x^2, \Delta t^2)$ (see eq. 99).

5.5. Perspective on LW operators

For the homogeneous case, the equivalence of the FDM-LW scheme and the optimally accurate O(2,2) FDM scheme (implemented as a predictor-corrector scheme) was proved by transforming the latter to a one-step explicit scheme. The equivalence between various one-step (LW) schemes and two-step (predictor-corrector) schemes is shown in Table 1

The two-step (predictor-corrector) algorithms seem to be somewhat preferable to one-step algorithms for the following reasons: (1) the localization of the stencils (compare eq. 18 of GT98 to eqs. 81 and 84, above), (2) the greater ease of programming for the heterogeneous 2-D and 3-D cases (see TG00), and (3) the greater ease of deriving the operators for boundary elements or heterogeneous media. The first point is especially important for massive parallel computing. As for the second point, the derivation of LW schemes for the heterogeneous 2-D or 3-D cases seems unnecessarily complex as compared to the predictor-corrector schemes (compare Sei and Symes, 1995, to GT98 or TG00).

6. Numerical Examples

In this section we present simple one-dimensional numerical examples to compare the effectiveness of three numerical schemes: (1) optimally accurate PSM-FDM, (2) optimally accurate second order FDM in space and time (hereafter referred to as FDM-FDM), and (3) a fourth-order optimally accurate PSM-RK4 scheme. The first and third of these schemes were presented above in sections 3 and 4 respectively, and the second scheme was presented by GT98 and is also summarized above in section 5.4. As shown above in section 5, the first and second schemes, which are two-step (predictor-corrector) schemes, are basically equivalent to the corresponding one-step (Lax-Wendroff) schemes.

Table 1
A comparison of the two-step (predictor-corrector scheme) optimally accurate schmes and the equivalent one-step Lax-Wendroff schemes

	Equivalence of schemes	
	Two-step predictor-corrector scheme	One step explicit scheme (LW)
PSM-FDM	· Section 2 of this paper optimally accurate PSM-FDM	· Kneib and Kerner (1993)
pure FDM	· GT98 1-D heterogeneous case · TG00 2-D and 3-D heterogeneous case	· Dablain (1986) 2-D ''Block'' heterogeneous case · Sei and Symes (1995) 2-D heterogeneous acoustic case · Igel et al. (1995) General anisotropic case · Blanch and Robertsson (1997) 1-D homogeneous visco-elastic case

Several studies (e.g., Kosloff et al., 1984, Cerjan et al., 1985, Kosloff and Kosloff, 1986, Furumura and Takenaka, 1995, Wu and Lees, 1997) have addressed the question of how to include boundary conditions such as a free surface or an absorbing boundary layer in PSM schemes, but we use only periodic boundary conditions in the calculations presented here.

6.1. Relative solution error in time domain

GT95 obtained a formula for the relative error of solutions obtained using optimally accurate numerical operators in the frequency domain (see eq. 4 above, and eq. 2.20 of GT95). For the optimally accurate PSM-FDM operators, the relative error in the frequency domain is given by eq. (43). In the time domain, the net solution error is proportional to Δt^2, where the proportionality constant K represents the weighted contribution of the various frequencies that are summed to obtain the solution:

$$\text{Relative error} \approx \frac{K^2(\beta\Delta t)^2}{12} \tag{109}$$

where we assume a homogeneous medium ($\beta =$ const.). K is determined by the frequency dependence of the problem, i.e. by the frequency content of the source. Assuming K in eq. (109) is a weighted contribution of the various frequencies, we can apply eq. (109) to the heterogeneous problem if viewed as an approximation that does not include errors due to aliasing.

If only the discretization error due to the FDM temporal differentiation were considered, it might appear that the error of the solutions obtained using the optimally accurate PSM-FDM scheme could be reduced to any arbitrary small level by using a sufficiently smaller time step. However the numerical examples presented below show that this is not the case, as there are other errors that must also be considered, in particular the aliasing of the PSM spatial derivatives due to velocity structures that include a sharp discontinuity (or a steep velocity gradient). As shown below, when the structure model has sharp discontinuities, the solution error for the PSM schemes is dominated by errors due to aliasing.

The solution error of an optimally accurate second-order (in both space and time) FDM scheme (GT98) is:

$$|\delta T_{mm}| = \frac{\omega_m^2\Delta t^2 + k_m^2\Delta x^2}{12}, \tag{110}$$

in the frequency domain and

$$\text{Relative error} \approx \frac{K^2\left(\Delta x^2 + (\beta\Delta t)^2\right)}{12} \tag{111}$$

in the time domain. By comparing eqs. (109) and (111), we see that the major difference between the optimally accurate PSM-FDM scheme and the opti-

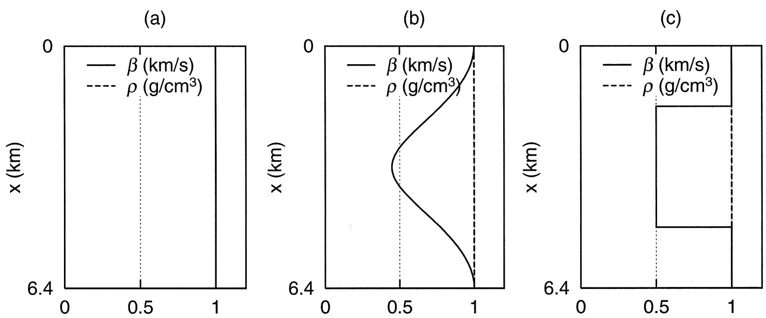

Fig. 1. Density and velocity structures for 1-D numerical computation test. (a) homogeneous model, (b) smoothly varying heterogeneous model ($\beta = \sqrt{0.6 + 0.4\cos(2\pi x/6.4)}$), and (c) discontinuous two-layered model. Density structures are constant for all models. All models are periodic in space, i.e., have periodic boundary conditions.

mally accurate FDM-FDM scheme is that the solution error of the latter depends on both the spatial and temporal grid spacing, while the solution error of the former depends only on the time step.

6.2. Performance comparison of conventional and optimally accurate PSM-FDM schemes

In this section, we compare the performance of the optimally accurate PSM-FDM scheme to the conventional PSM-FDM scheme. We consider three 1-D problems: the homogeneous structure shown in Fig. 1a, the smoothly varying heterogeneous structure shown in Fig. 1b, and the heterogeneous structure with sharp discontinuities shown in Fig. 1c. The length of the computational domain is 6.4 km, and the structure and wavefield repeat periodically. The source is a single force with a Ricker wavelet time-dependence whose central frequency is 0.6 s. The source is at $x = 3.2$ km and the receiver is at $x = 4.0$ km. We calculate waveforms with a duration of 11.2 s, which is roughly the time required for a wave to travel about two laps in the computational domain. The discontinuities for the structure shown in Fig. 1c are located exactly at a grid point.

Fig. 2 shows the relation between the time step and the PSM-FDM solution error for the case of $N = 512$ spatial grid intervals. The horizontal axis is the timestep Δt normalized by the FDM Courant limit:

$$\Delta t_{\mathrm{Courant}} = \frac{\Delta x}{\beta_{\max}}, \tag{112}$$

where $\beta_{\max}$ is the maximum velocity in the medium. The relative solution error is defined as

$$\text{relative solution error}[\%] = \sqrt{\frac{\int (u - u_{\mathrm{exact}})^2 dt}{\int u_{\mathrm{exact}}^2 dt}} \times 100. \tag{113}$$

For the homogeneous case (Fig. 1a) and the discontinuous two-layered case (Fig. 1c), u_{exact} is the analytical solution for a point source, while for the smoothly heterogeneous case (Fig. 1b), u_{exact} is the numerical solution for a fine grid ($N = 8192$).

For the homogeneous case (Fig. 2a), the errors decrease as we take smaller time steps. As theoretically expected, the solution error is proportional to Δt^2 for the PSM-FDM schemes. When the time step is very small and the optimally accurate PSM-FDM scheme is used, the solution error is saturated because of the aliasing due to the point source term.

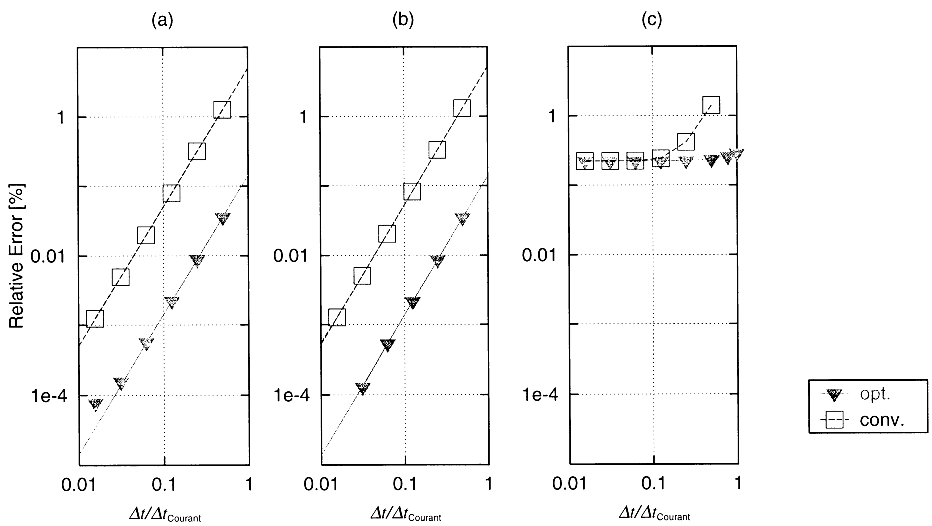

Fig. 2. Time domain relative error of waveforms computed by the conventional (squares with chained line) and optimally accurate (gray triangles with solid line) PSM-FDM operators with $N = 512$ spatial grid points. Time step is normalized by the Courant stability limit of a pure FDM scheme. (a), (b) and (c) correspond to the structures shown in Fig. 1a, 1b, and 1c respectively. The solid and dotted lines are plotted by empirical curve fitting.

Except for this saturation, the solution error of the synthetics computed by the optimally accurate PSM-FDM operators is about 35 times less than that for the synthetics computed by the conventional PSM-FDM operators for the same spatial and temporal grid, while the CPU time is about only twice that of the conventional operators (see section 3.3). The saturation due to the point source term is not important for the conventional PSM-FDM scheme, but for highly accurate PSM-FDM schemes such as optimally accurate PSM-FDM or PSM-RK4 schemes, this saturation becomes important. For the smoothly varying heterogeneous case (Fig. 2b), the error decreases as smaller time steps are used, as for the homogeneous case, and the solution error of the optimally accurate operators is smaller than that of the conventional operators.

In contrast, the saturation of the solution error is pronounced for the structure which has a sharp discontinuity (Fig. 2c). This saturation is not due to the point source term but rather to the inability of Fourier (FFT) differentiation to accurately account for the effect of the sharp discontinuities in the structure. The Fourier (FFT) derivative operators have large errors due to aliasing, even though the discontinuity is located precisely at a grid point. For the optimally accurate PSM-FDM computation, the error remains essentially unchanged as the time step is decreased from its stability limit ($0.78\,\Delta t_{\text{Courant}}$), while for the conventional scheme saturation occurs when the time step is smaller than about $0.1\,\Delta t_{\text{Courant}}$. Thus the optimally accurate PSM-FDM scheme achieves the same accuracy as the conventional PSM-FDM scheme with about eight times as large a time step. This means that the optimally accurate scheme is about four times more cost-effective than the conventional schemes, after taking into account the additional computations.

6.3. Comparison of time-domain schemes

The error of PSM-FDM schemes can be reduced by either using a finer mesh or using a smaller time step, but both will increase the CPU time. We investigate their relative cost-effectiveness in improving the accuracy of the numerical solution, and show below that the answer depends on the nature of the velocity model.

The relation between the CPU time and the relative solution error in the time domain of the optimally accurate PSM-FDM scheme is shown in Fig. 3 for the three velocity structures in Fig. 1. The error due to the point source is ignored for the PSM-based schemes. Fig. 3a shows that the efficiency of the PSM-FDM for the homogeneous case can best be improved by decreasing the time step without using

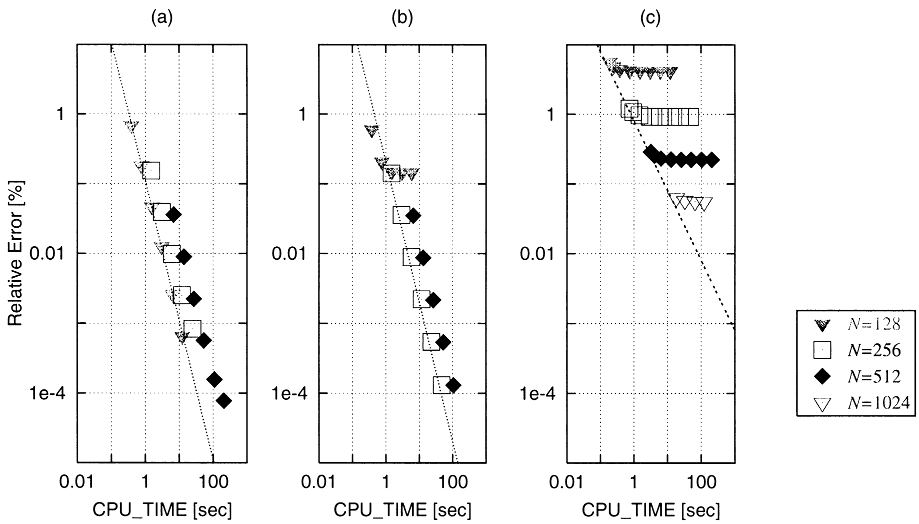

Fig. 3. The CPU time versus time domain relative error of the optimally accurate PSM-FDM scheme for the structures in Fig. 1. The different symbols represent different spatial gridding. For each given type of symbol, the time step Δt decreases from the left to the right. The dotted lines show the most cost-effective choice for each scheme.

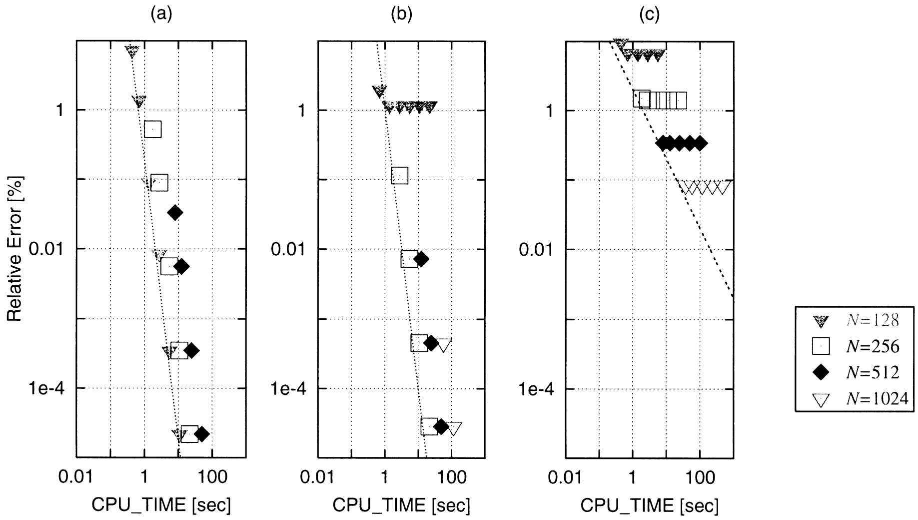

Fig. 4. The CPU time versus time domain relative error for the PSM-RK4 scheme (same format as Fig. 3).

a finer mesh. Thus the most cost-effective strategy for the PSM-FDM scheme for the homogeneous case is to decrease the time step, while using the coarsest possible spatial grid (at least two grid points per wavelength).

For the smoothly heterogeneous case (Fig. 3b), the pattern is generally the same as for the homogeneous case. Note, however, that the coarsest grid ($N = 128$) is insufficient, as shown by the fact that the error saturates as Δt decreases. In contrast, for the structure which has sharp discontinuities (Fig. 3c), the solution error saturates for all values of N. This is because the solution error for a structure which has a sharp discontinuity is dominated by aliasing error due to the sharp discontinuity. The only way to improve the accuracy for this case is to use a smaller spatial grid, since, as shown in Fig. 3c, there is no appreciable advantage to decreasing the time step.

The relation of the CPU time and relative solution error of the PSM-RK4 scheme (Fig. 4) is similar to that of the optimally accurate PSM-FDM scheme,

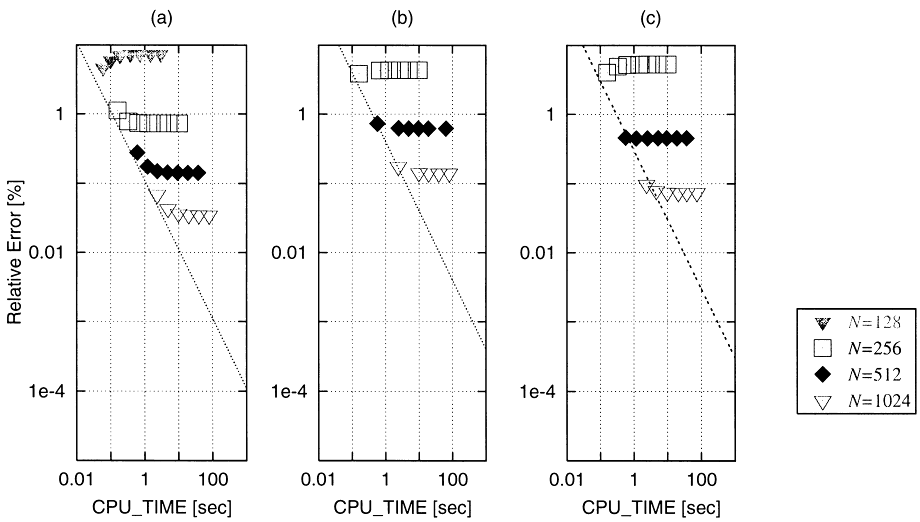

Fig. 5. The CPU time versus time domain relative error for the optimally accurate $O(2,2)$ FDM scheme (same format as Fig. 3).

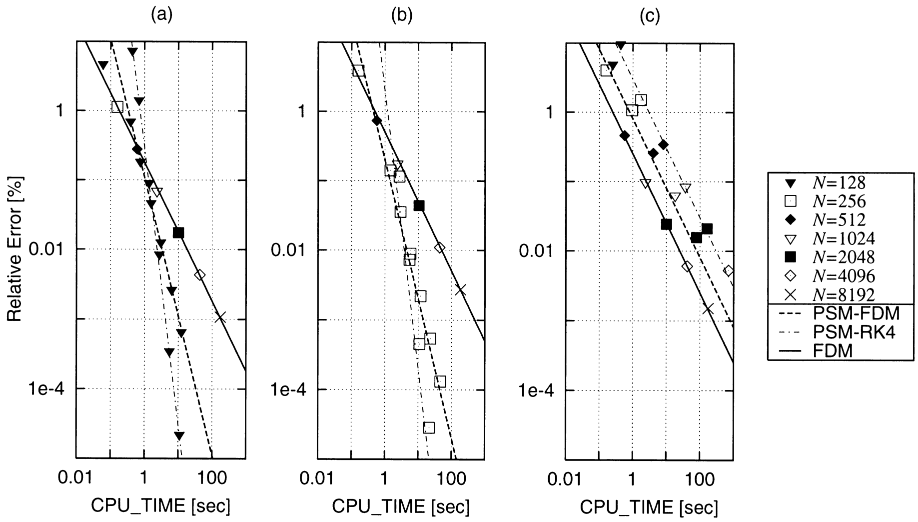

Fig. 6. The CPU time versus time domain relative error for three different structures. The results for the optimally accurate PSM-FDM scheme (thick dotted line), PSM-RK4 (thin dotted line) and optimally accurate $O(2,2)$ FDM (thick solid line) are plotted. Only the most cost-effective choice for each scheme and grid spacing is plotted.

but the error of the PSM-RK4 scheme is proportional to Δt^4 for the homogeneous (Fig. 4a) and smoothly heterogeneous media (Fig. 4b). For the structure which has sharp discontinuities (Fig. 4c), as was also the case for the optimally accurate PSM-FDM schemes, the error is determined mainly by the spatial grid interval.

The relative solution error of the optimally accurate $O(2,2)$ FDM scheme (Figs. 5a–c) depends on both the temporal and spatial gridding. For all cases, the solution error is dominated by the $O(\Delta x^2)$ error. The slopes of the lines in the three figures (Figs. 5a–c) are all equal to -1. This is because for a time step near the Courant limit, both the relative solution error and the CPU time for a 1-D calculation are proportional to N^2. Note that the slopes would be respectively $2/3$ and $2/4$ for 2-D and 3-D calculations, as the CPU times would be proportional to N^3 and N^4 respectively.

The best results for the PSM-FDM, the PSM-RK4, and $O(2,2)$ FDM schemes are shown in Fig. 6 for (a) the homogeneous case, (b) the smoothly heterogeneous case and (c) the discontinuous case. For the homogeneous and the smoothly heterogeneous cases, the most cost-effective scheme is the PSM-RK4 scheme, whose relative error is roughly proportional to the fourth power of the CPU time.

For the structure which has sharp discontinuities, the most cost-effective of the three schemes is the optimally accurate $O(2,2)$ FDM scheme. The reason is that the relative error of PSM-based schemes for this case is of the same order as that of an $O(2,2)$ FDM scheme with the same grid spacing, despite the smaller computational requirements per grid point of the FDM scheme. Thus the $O(2,2)$ FDM scheme is the most cost-effective scheme for the discontinuous case. We did not compare the PSM-RK4 scheme to other higher order time-integration scheme such as that of Tal-Ezer et al. (1987) or Igel et al. (1995). However the performance of all such higher-order schemes for media with sharp discontinuities is limited by the aliasing of the spatial PSM scheme, rather than by the error of the time-integration scheme.

7. Discussion

PSM schemes have sometimes been characterized as superior to FDM schemes from the standpoint of both memory and CPU time. However, the results presented in this paper show that the choice of method depends heavily on the nature of the problem. As the Earth has sharp discontinuities at the free surface and at internal discontinuities, and also has sharp velocity gradients, optimally accurate $O(2,2)$ FDM schemes are likely to be more cost-effective schemes for most practical applications. The difficulties of handling non-periodic boundary conditions, and the non-locality of memory access of the FFT, which seem to make PSM schemes difficult to implement on massively parallel computers (Furumura et al., 1998) compared with FDM schemes, are further arguments against the use of PSM-based methods in practical applications.

7.1. Relation between grid spacing and accuracy

It is apparently widely believed (e.g. Fornberg, 1996) that only two grid points per wavelength are sufficient for PSM-based schemes to achieve sufficient accuracy, but as shown by the above examples, this is not true for structures that have sharp discontinuities. On the other hand, to determine the number of grid points per wavelength required for an optimally accurate (second order in space and time) FDM scheme to achieve some given desired accuracy, we can use eq. (6.2) in GT95. Note that the criterion for accuracy is the relative error of the numerical solution, rather than the numerical dispersion of the phase velocity.

For a monochromatic wave and a 1-D homogeneous medium, the relative error is given by eq. (111).

$$\begin{aligned}\text{relative error} &= \frac{k_x^2 \Delta x^2 (1+\mathcal{C}^2)}{12}\\ &= \frac{(2\pi)^2(1+\mathcal{C}^2)}{12}\frac{\Delta x^2}{\lambda^2}\\ &\approx \frac{6.6}{(\text{grid points/wavelength})^2},\end{aligned} \tag{114}$$

where $\lambda = 2\pi/k_x$, and the Courant limit ($\mathcal{C} = 1$) is used. The grid spacing required to produce some given desired relative error is therefore:

$$\text{grid points/wavelength} \approx \sqrt{\frac{6.6}{\text{relative error}}}. \tag{115}$$

Thus to achieve a relative error of $0.01 = 1\%$ using optimally accurate $O(2,2)$ time domain FDM operators for a 1-D problem, we require about 25 grid points/wavelength. If a coarser grid, say 8 points per wavelength, is used, a solution error of about 10% would be obtained. For a general heterogeneous medium, the relative error cannot be rigorously estimated. However we can use the above result as a rough estimate.

Previous workers appear not to have sufficiently considered the question of what level of relative error of the numerical solution was acceptable in various applications (e.g. waveform inversion), as they have used the error of the phase velocity as the criterion for accuracy. This appears to have led to overly optimistic expectations that relatively coarse grids would yield acceptable results for practical applications. We suggest that users of numerical modeling codes should carefully consider this question when choosing their grid spacing.

Acknowledgements

We thank Johan O.A. Robertsson for valuable comments that greatly contributed to improving the manuscript. We also thank one anonymous reviewer for helpful comments. This research was partly supported by a grant from the Japanese Ministry of Education, Science and Culture (No. 10640403). H.M. and N.T. were supported by JSPS Fellowships for Young Scientists.

Appendix A. Optimally accurate PSM-FDM schemes for 2-D and 3-D case

The conventional PSM-FDM operator for the equation of motion is

$$\begin{array}{|c|c|}\hline & x,y,z \\ \hline t+\Delta t & \rho \\ t & -2\rho \\ t-\Delta t & \rho \\ \hline\end{array}\ \mathbf{u}_i - \begin{array}{|c|c|}\hline & x,y,z \\ \hline t+\Delta t & \\ t & \mathcal{D}_j C_{ijkl} \mathcal{D}_l \\ t-\Delta t & \\ \hline\end{array}\ \mathbf{u}_k = \mathbf{f}_i, \tag{A1}$$

where $\mathcal{D}$ is the Fourier differentiation operator with respect to the i-th spatial component, $\mathbf{u}_i$ is i-th component of displacement rather than eigenmode, C_{ijkl} is the elastic modulus, and summation over repeated indices is implied.

Neglecting the numerical error due to aliasing of the Fourier difference operator $\mathcal{D}$, the optimally accurate operator for this case is the following:

$$\begin{array}{|c|c|} \hline & x,y,z \\ \hline t+\Delta t & \rho \\ t & -2\rho \\ t-\Delta t & \rho \\ \hline \end{array}\ \mathbf{u}_i - \begin{array}{|c|c|} \hline & x,y,z \\ \hline t+\Delta t & \frac{1}{12}\mathcal{D}_j C_{ijkl}\mathcal{D}_l \\ t & \frac{10}{12}\mathcal{D}_j C_{ijkl}\mathcal{D}_l \\ t-\Delta t & \frac{1}{12}\mathcal{D}_j C_{ijkl}\mathcal{D}_l \\ \hline \end{array}\ \mathbf{u}_k = \mathbf{f}_i. \qquad (A2)$$

The stability condition for the 2-D and 3-D case is derived in the same way as for the 1-D case (Kosloff and Baysal, 1982, Kosloff et al., 1984, Witte and Richards, 1990). The stability condition cannot be derived analytically for the general heterogeneous case, but can be derived for the homogeneous case with periodic boundary condition. Omitting details and assuming $\Delta x = \Delta y = \Delta z$, the stability conditions of the conventional PSM-FDM operators for the 2-D and 3-D case are

$$\Delta t \leq \frac{\sqrt{2}}{\pi}\frac{\Delta x}{V_{\max}} \approx 0.45\frac{\Delta x}{V_{\max}}, \qquad (A3)$$

and

$$\Delta t \leq \frac{2}{\sqrt{3}\,\pi}\frac{\Delta x}{V_{\max}} \approx 0.36\frac{\Delta x}{V_{\max}} \qquad (A4)$$

respectively, where $V_{\max}$ is the maximum velocity of the system. For the SH-problem, $V_{\max} = V_s$, and for P-SV problem, $V_{\max} = V_p$. The stability conditions of the optimally accurate PSM-FDM operators for 2-D and 3-D case are

$$\Delta t \leq \frac{\sqrt{3}}{\pi}\frac{\Delta x}{V_{\max}} \approx 0.55\frac{\Delta x}{V_{\max}}, \qquad (A5)$$

and

$$\Delta t \leq \frac{\sqrt{2}}{\pi}\frac{\Delta x}{V_{\max}} \approx 0.45\frac{\Delta x}{V_{\max}}. \qquad (A6)$$

respectively. As was true for the 1-D case, the stability condition is slightly relaxed for the optimally accurate scheme as compared to the conventional scheme.

References

Blanch, J.O., Robertsson, J.O.A., 1997. A modified Lax-Wendroff correction for wave propagation in media described by Zener elements. Geophys. J. Int. 131, 381–386.

Cerjan, C., Kosloff, D., Kosloff, R., Reshef, M., 1985. A nonreflecting boundary condition for discrete acoustic and elastic wave equations. Geophysics 50, 705–708.

Cummins, P.R., Geller, R.J., Hatori, T., Takeuchi, N., 1994. DSM complete synthetic seismograms: SH, spherically symmetric, case. Geophys. Res. Lett. 21, 533–536.

Cummins, P.R., Takeuchi, N., Geller, R.J., 1997. Computation of complete synthetic seismograms for laterally heterogeneous models using the Direct Solution Method. Geophys. J. Int. 130, 1–16.

Dablain, M.A., 1986. The application of high-order differencing to the scaler wave equation. Geophysics 51, 54–66.

Daudt, C., Braile, L., Nowack, R., Chiang, C., 1989. A comparison of finite-difference and Fourier method calculations of synthetic seismograms. Bull. Seism. Soc. Amer. 79, 1210–1230.

Fornberg, B., 1987. The pseudospectral method: Comparisons with finite differences for the elastic wave equation. Geophysics 52, 483–501.

Fornberg, B., 1990. High-order finite differences and pseudo-spectral method on staggered grids. SIAM J. Numer. Anal. 27, 904–918.

Fornberg, B., 1996, A practical guide to pseudospectral methods, Cambridge University Press.

Frankel, A., Clayton, R.W., 1986. Finite difference simulations of seismic scattering: implications for the propagation of short-period seismic waves in the crust and models of crustal heterogeneity. J. Geophys. Res., 91, 6645–6489.

Furumura, T., Takenaka, H., 1995. A wraparound elimination technique for the pseudospectral wave synthesis using an antiperiodic extension of the wavefield. Geophysics 60, 302–307.

Furumura, T., Kennett, B.L.N., Takenaka, H., 1998. Parallel 3-D pseudospectral simulation of seismic wave propagation. Geophysics 63, 279–288.

Geller, R.J., Ohminato, T., 1994. Computation of synthetic seismograms and their partial derivatives for heterogeneous media with arbitrary natural boundary conditions using the Direct Solution Method. Geophys. J. Int. 116, 421–446.

Geller, R.J., Takeuchi, N., 1995. A new method for computing highly accurate DSM synthetic seismograms. Geophys. J. Int. 123, 449–470.

Geller, R.J., Takeuchi, N., 1998. Optimally accurate time domain second-order finite difference scheme for the elastic equation of motion: 1-D case. Geophys. J. Int. 135, 48–62.

Igel, H., Mora, P., Riollet, B., 1995. Anisotropic wave propagation through finite-difference grids. Geophysics 60, 1203–1216.

Kelly, K.R., Ward, W., Treitel, S., Alford, R.M., 1976. Synthetic seismograms: A finite difference approach. Geophysics 41, 2–27.

Kneib, G., Kerner, C., 1993. Accurate and efficient seismic modeling in random media. Geophysics 58, 576–588.
Kosloff, D., Baysal, E., 1982. Forward modeling by a Fourier method. Geophysics 47, 1402–1412.
Kosloff, D., Reshef, M., Lowenthal, D., 1984. Elastic wave calculations by the Fourier method. Bull. Seism. Soc. Amer. 74, 875–891.
Kosloff, R., Kosloff, D., 1986. Absorbing boundaries for wave propagation problems. J. Comp. Phys. 63, 363–376.
Lax, P.D., Wendroff, B., 1964. Difference schemes for hyperbolic equations with high order of accuracy: Comm. Pure Appl. Math 17, 381–398.
Levander, A.R., 1988. Fourth-order finite-difference P-SV seismograms. Geophysics 53, 1425–1436.
Özdenvar, T., McMechan, G., 1996. Causes and reduction of numerical artefacts in pseudo-spectral wavefield extrapolation. Geophys. J. Int. 126, 819–828.
Robertsson, J.O.A., Blanch, J.O., Symes, W.W., 1994. Viscoelastic finite-difference modeling, Geophysics 59, 1444–1456.
Sei, A., Symes, W., 1995. Dispersion analysis of numerical wave propagation and its computational consequences. J. Sci. Comput. 10, 1–27.
Takeuchi, N., Geller, R.J., 2000. Optimally accurate second-order time-domain finite difference scheme for computing synthetic seismograms in 2-D and 3-D media. Phys. Earth Planet. Int. 119, 103–138.
Takeuchi, N., Geller, R.J., Cummins, P.R., 1996. Highly accurate P-SV complete synthetic seismograms using modified DSM operators. Geophys. Res. Lett. 23, 1175–1178.
Tal-Ezer, H., Kosloff, D., Koren, Z., 1987. An accurate scheme for seismic forward modelling. Geophys. Prospect. 35, 479–490.
Witte, D.C., Richards, P.G., 1990. The pseudospectral method for simulating wave propagation. Comp. Acoust. 3, 1–18.
Wu, H., Lees, J., 1997. Boundary conditions on a finite grid: Applications with pseudospectral wave propagation. Geophysics 62, 1544–1557.